Available online at www.jourcc.com

Journal homepage: www.JOURCC.com

Journal of Composites and Compounds

A comparative investigation on the analytical properties and nanostructure of the Sargelu and Asmari reservoirs

Wenjun He [a], Yamin Wang [b], Liang Zhong [c], Seyed Ali Delbari [d], Abbas Sabahi Namini [d], Dokyoon Kim [e,f], Ho Won Jang [g], Mohammadreza Shokouhimehr [f,g]**

[a] 1 Research Institute of Exploration and Development, PetroChina Xinjiang Oilfield Company, Karamay, China.
[b] Institute of Energy, Peking University, Beijing, China.
[c] Operation Area of Fengcheng Oilfield, PetroChina Xinjiang Oilfield Company, Karamay, China.
[d] Department of Engineering Sciences, Faculty of Advanced Technologies, University of Mohaghegh Ardabili, Ardabil, Iran.
[e] Department of Bionano Engineering, Hanyang University, Ansan 15588, Republic of Korea.
[f] Institute of Nanosensor Technology, Hanyang University, Ansan 15588, Republic of Korea.
[g] Department of Materials Science and Engineering, Research Institute of Advanced Materials, Seoul National University, Seoul 08826, Republic of Korea.

ABSTRACT

The objective of this research was to gain insight into the composition and nanostructure of two shale formations, Sargelu and Asmari. Among the techniques used are X-ray diffractometry (XRD), X-ray fluorescence (XRF), thermogravimetric analysis (TGA), field emission scanning electron microscopy (FESEM), Fourier-transform infrared spectroscopy (FTIR), FESEM focused ion beam (FIB), and transmission electron microscopy (TEM). According to the XRD results, the main components of both shales were calcite, quartz, and kaolinite. CaO, SiO_2, and Fe_2O_3 were the most common components in both reservoirs, according to the XRF analysis, while P_2O_5, SrO, and MoO_3 were only found in the Asmari formation. According to the TGA study, organic matter and other probable carbonate components comprised 37% of the Sargelu and 40.5% of the Asmari shales. The organic functional groups were detected using FTIR in both samples. Subsequently, various microscopy techniques were utilized to examine different pores, cracks, and nanostructures in each formation.

Peer review under responsibility of UGPH.

ARTICLE INFORMATION

Article history:
Received 06 April 2023
Received in revised form 18 May 2023
Accepted 29 May 2023

Keywords:
Shale
Reservoir
Nanostructure
Analysis
Characterization
Scanning electron microscopy

1. Introduction

Shale gas has become recognized as a reliable unconventional hydrocarbon resource, with numerous researchers worldwide, especially in North America and China, working on it. For years, mudrocks and shale rocks containing organic matter (OM) were considered source rocks, gradually supplanting the conventional petroleum industry. However, the commercialization of shale oil and gas extraction techniques has altered the perspective of shale reservoirs as viable hydrocarbon reserves [1-5]. One of the main challenges in shale technology is drilling shale formations, which results in high operating cost. The complex chemical and physical interactions between drilling fluid and shale rocks may lead to sloughing, plastic flow, dispersion, swelling, and other issues that may be addressed with suitable solutions such as selecting the appropriate well trajectory, mud weight, drilling fluid hydraulic, and designing a hindering drilling fluid [6-10]. Indeed, obtaining comprehensive information on pore characteristics in shale rocks, such as pore size distribution and porosity, appears to be essential to assessing the reservoir's potential and achieving effective exploitation. This is because these characteristics determine the amount of space there is within the shale rock [11-15].

In shale rocks, there are three distinct varieties of gas: free gas in the pores and fractures, dissolved gas in the oil and water, and adsorbed gas in the OM and inorganic minerals [16]. As a result, it is important to investigate the shale pores in terms of geometry (size, distribution, and shape) and topology (connectivity, fractality, and tortuosity) [17]. Small pores have a great surface area and adsorption potential energy compared with large pores. Consequently, when pore diameters vary, different adsorption behaviors and adsorbed gas ratios are expected. Micropores are generally abundant in shale rock, while macropores have the smallest fraction [18–20].

A number of different techniques can be used to determine the porosity of a shale formation, in addition to its composition. Many investigations have utilized conventional methods to characterize shales, including mercury injection capillary pressure, small-angle neutron scattering,

* Corresponding author: Yamin Wang; E-mail: yamin.wang@pku.edu.cn, Mohammadreza Shokouhimehr; Email: rezamehr2023@gmail.com

https://doi.org/10.61186/jcc.5.2.1

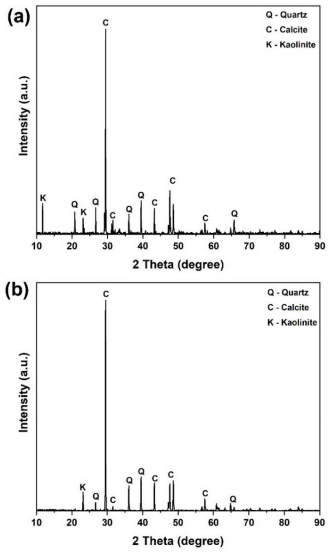

Fig. 1. XRD patterns of (a) Sargelu, and (b) Asmari reservoirs.

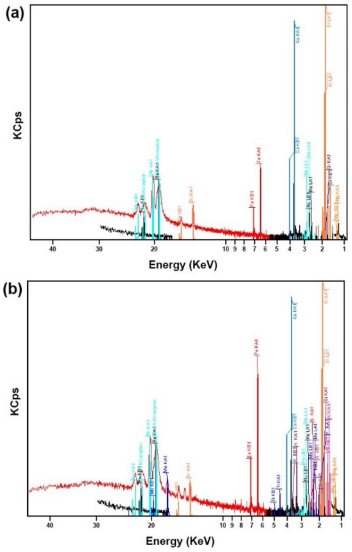

Fig. 2. XRF spectra of (a) Sargelu, and (b) Asmari reservoirs.

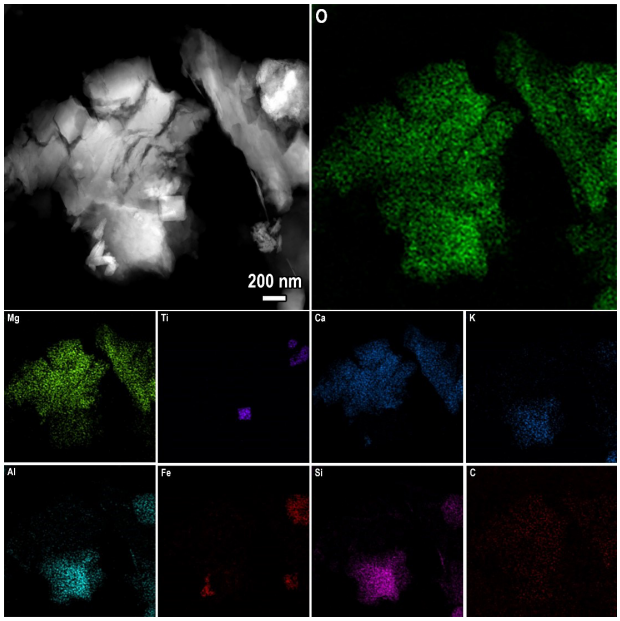

Fig. 3. STEM image and EDS elemental mapping of Sargelu reservoir.

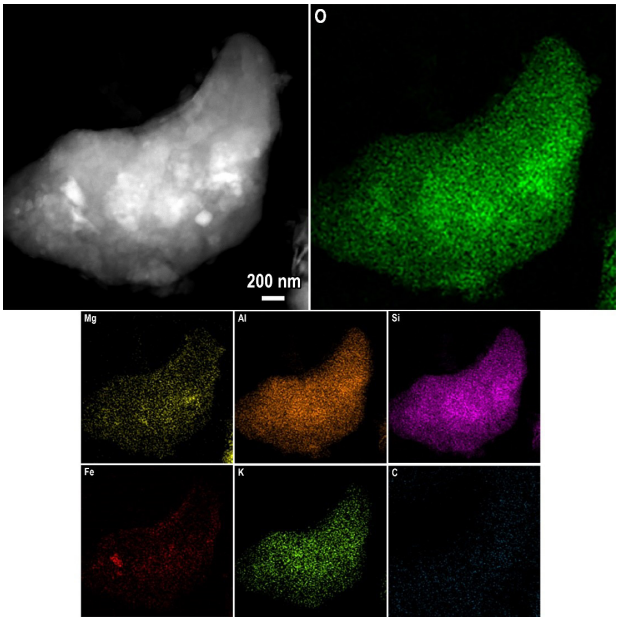

Fig. 4. STEM image and EDS elemental mapping of Asmari reservoir.

ultra-small-angle neutron scattering, and field emission scanning electron microscopy (FESEM) [21–23]. Furthermore, X-ray diffractometry (XRD) and Fourier-transform infrared spectroscopy (FTIR) have been used to investigate the composition of the shale rock and OM [24–27]. However, the precise structural and morphological distribution of materials with three-dimensional frameworks at the micro/nanoscale is revealed using the most recent analytical and characterization methods.

We conducted a comparison analysis of the Sargelu and Asmari formations in terms of nanostructure and chemical composition. Various techniques, including focused ion beam (FIB), high resolution transmission electron microscopy (HRTEM), X-ray fluorescence (XRF), XRD, FTIR, FESEM, FESEM-FIB, and thermogravimetric analysis (TGA), were utilized in this study to precisely analyze the shale specimens. The information provided in this research can be useful to researchers working in this area because there is a lack of practical information on these formations.

2. Experimental and methods

The bulk samples were polished to have a smooth surface, and the powder samples were ground to ~80 mesh size for the analytical assessments. The presence of minerals in the specimens was investigated using an XRD instrument (D8-Advance Bruker). Furthermore, utilizing the XRF (Shimadzu 1800) technique, a precise evaluation of the likely chemicals in the rocks was performed. The hydrocarbon content of the samples was determined using the TGA (TA Instruments Discovery) approach. This test was carried out at temperatures ranging from 20 to 900 °C (at a rate of 10 °C/min). An FTIR device was used to examine the chemical bonding of the shale specimens (Thermo Fisher Scientific Nicolet iS50). To examine the framework of the shales, various microscopy techniques such as FESEM-FIB, and HRTEM were used. A JEOL JEM-2100F microscope with an energy-dispersive X-ray spectroscopy (EDS) detector was used to collect TEM images.

3. Geological setting

The Zagros fold zone has 14 kilometers of sediments ranging in age from the Palaeozoic to the Quaternary. Carbonate sediments are regularly formed in the Fars geological area from the upper Paleozoic to the tertiary periods. The Lorestan geological area (Lorestan is a province

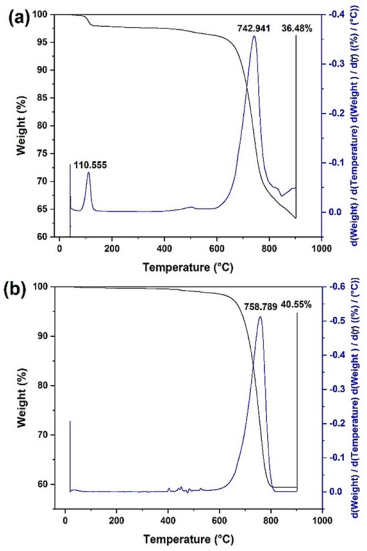

Fig. 5. TGA analysis results of (a) Sargelu, and (b) Asmari reservoirs.

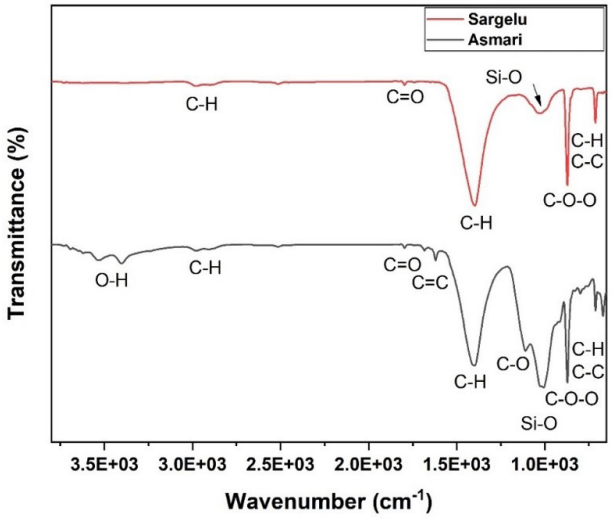

Fig. 6. FT-IR spectra of Sargelu and Asmari reservoirs.

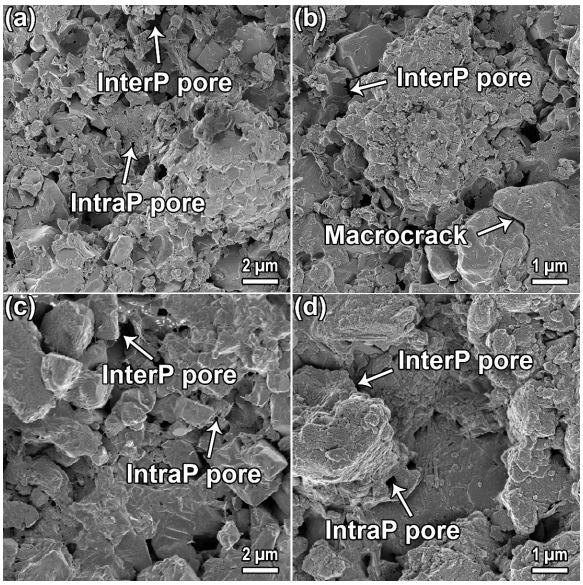

Fig. 7. FESEM images of (a, b) Sargelu and (c,d) Asmari reservoirs.

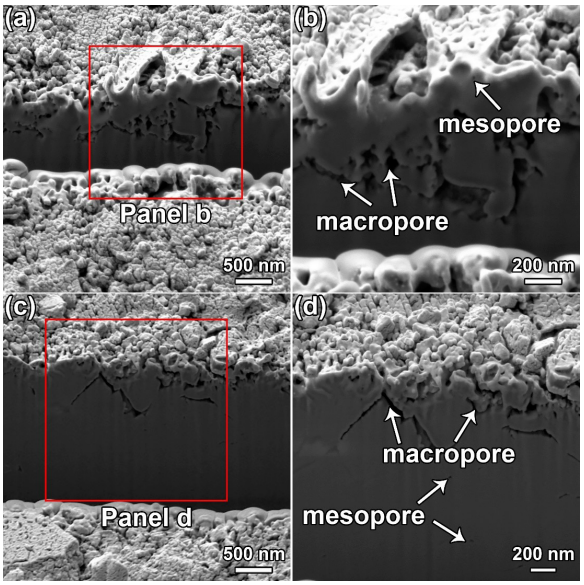

Fig. 8. In situ FESEM-FIB images of (a, b) Sargelu and (c,d) Asmari reservoirs.

in southwest Iran's Zagros Mountains chain) contains the lowest part of the sedimentary basin, where shale facies and pelagic limestone are abundant. The central Zagros area, which includes the Dezful embayment, which is positioned between the deep basins of the Lorestan and Fars platforms, demonstrates multiple sea regressions and progressions due to alternating carbonate and shale strata deposited in this area [28]. The Sargelu formation is a Middle Jurassic formation that sits beneath and overlies the Najmeh formation (below a discontinuity surface). The lithology of this formation is dominated by brown lime and bituminous gray shale, with infrequent appearances of brown and calcareous dolomites. The Sargelu formation in southwest Iran is a source rock with a high potential for the production of hydrocarbons because of the reductive environmental circumstances present at the time of deposition [29,30].

The Asmari formation can be found in the Zagros basin, but it is especially well-developed in the Dezful embayment. Many stages of sandstone deposits are interspersed with Asmari carbonate strata in the south of the Dezful embayment. The Asmari formation consists of 380 m thick to large carbonate layers and a siliciclastic succession classified into five zones according to petrophysical properties. Zone 1 is the deepest zone, overlying the Pabdeh formation's shale and marls, and zone 5 is the largest below the cap rock (Gachsaran formation). The lower boundary of the Asmari formation is gradational with the Pabdeh formation, but it has a firm upper boundary with the Gachsaran formation. In the Aghajari oilfield, the Asmari formation is estimated to have originated during the Chattian-Burdigalian eras as a carbonated homoclinal ramp [31, 32].

4. Results and discussion

Various techniques have been used to investigate the composition of both reservoirs. The XRD analysis findings of the shale rocks are shown in Fig. 1. As can be seen, the primary gradients in both samples are essentially comparable. Calcite is the most abundant mineral in both samples, but quartz and kaolinite are also present. Fereidoni and colleagues [33] performed a primary study on the composition of the Sargelu formation. They reported the presence of various compounds in the investigated rocks, such as calcite, quartz, illite, and dolomite. Furthermore, they evaluated a basic investigation on the chemical composition of the Asmari formation, reporting the presence of the mineral's calcite, quartz, dolomite, illite, chlorite, and pyrite [34]. We applied the XRF technique to examine the chemical composition of the shale spec-

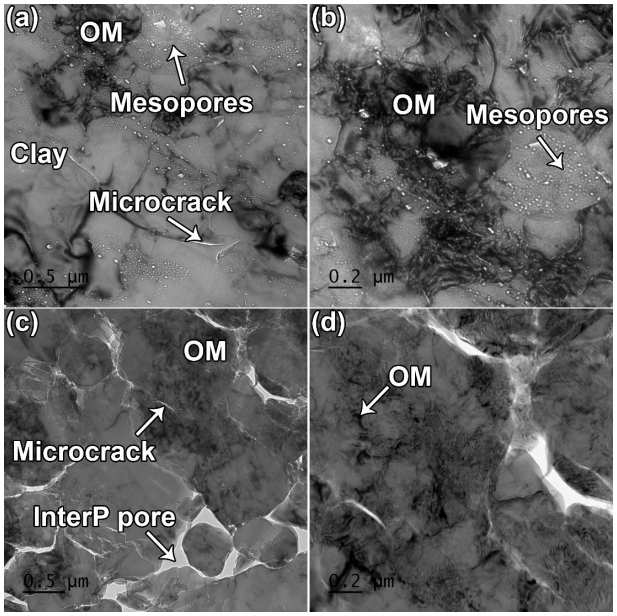

Fig. 9. TEM images of FIB milled (a, b) Sargelu and (c,d) Asmari reservoirs.

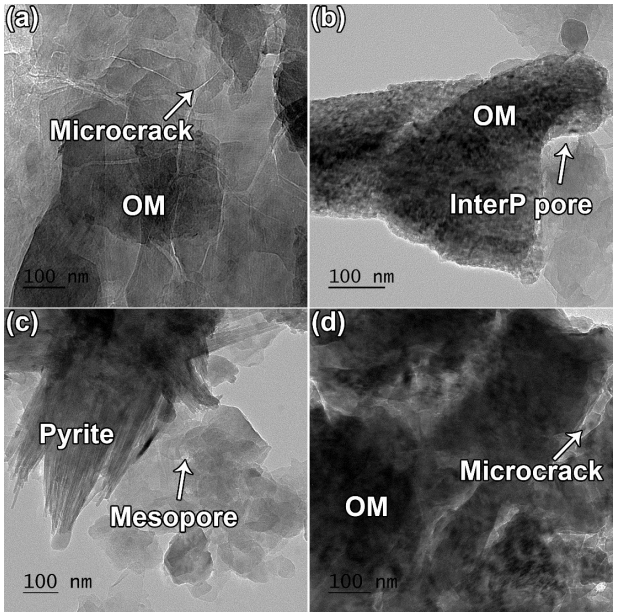

Fig. 10. TEM images of (a, b) Sargelu and (c,d) Asmari reservoirs in powder form.

imen and estimated the probable chemicals in the rock; the findings are shown in Fig. 2 and Table 1. CaO comprises ~45% of the Sargelu sample, while it makes up more than 80% of the Asmari rock. Other minerals present in both formations include SiO_2, Al_2O_3, Fe_2O_3, K_2O, MgO, and TiO_2. However, P_2O_5, SrO, and MoO_3 were all only discovered in Sargelu sample. The scanning TEM (STEM) image and EDS map analyses of the samples (in powder form) are shown in Figs. 3 and 4 and are consistent with the compositional data. The distribution of various elements in each reservoir can be investigated using these elemental maps.

Fig. 5 depicts the results of the TGA analysis for both samples. As can be seen, the Sargelu formation has 36.48% carbonate species, but the Asmari reservoir contains more than 40% organic species or other likely constituents. According to both representations, the breakdown process begins at 600 °C and progresses to temperatures ~750 °C. Fig. 6 illustrates the FTIR spectra of two samples. Stretching aliphatic bonds (CH_3 + CH_2) can be detected at 2800 and 1400 cm^{-1} in both formations. The appearance of C=O peaks at 1800 cm^{-1} confirms the presence of carbonyl and carboxyl groups. Si-O bonds are related with the peaks at 1031 cm^{-1} (Sargelu) and 1019 cm^{-1} (Asmari). In both samples, there are two sharp peaks at 874 that reflect CO_3^{2-}. Furthermore, the vibrations of C-C (700-400 cm^{-1}) and aromatic C-H (900-700 cm^{-1}) are responsible for the 400-900 cm^{-1} peaks. Some peaks, however, can only be seen in Asmari rocks and not Sargelu sample. Those in the 3408-3533 cm^{-1} range demonstrate the existence of OH^- groups, in addition to inter-layer and/or structural water inside some minerals. The presence of carbon-carbon double bonds (C=C), known as alkenes, is suggested by the peak at 1620 cm^{-1}. Finally, the C-O stretch peak at 1119 cm^{-1} is related to the Asmari formation's Alkyl group [35-39].

Fig. 7 shows FESEM micrographs of the Sargelu and Asmari reservoirs at different magnifications. Both samples have nearly the same type of pores. Pores are classified as either intraparticle (intraP) or interparticle (interP) pores based on where they develop. When some buried and unstable minerals, such as carbonate, quartz, and calcite, dissolve, intraP holes occur between the mineral layers and dissolution pores. This sort of pore is common in shale reservoirs and can be found between aggregates and minerals. They typically have a polygonal or elongated form. Because these pores are greater than 50 nm in diameter, they play an essential role in OM storage [40]. Furthermore, macrocracks can be seen within the microstructure of the shale samples studied. The permeability of the shale reservoir would be greatly increased if mesopores and micropores could be linked to these macrocracks via microfractures, as shown in the TEM images below. Additionally, in-situ FESEM-FIB images of both shale reservoirs are shown in Fig. 8. Despite the presence of numerous interP and intraP pores in both samples, it appears that the Sargelu sample has a larger volume percentage of porosity than the Arsmari. The Sargelu formation has defined shape in terms of pore interconnectivity. As is well-known, OMs can be removed more easily when the formation is porous with interconnecting pores.

Fig. 9 depicts TEM images of FIB milled samples of the Sargelu and Asmari reservoirs (in film forms). Some observations can be made by comparing these micrographs. To begin with, the distribution of OMs in the Asmari rocks is more uniform than in the Sargelu. In other words, some sections of the Sargelu formation have collected OMs, but they appear to be distributed uniformly across the shale. In terms of pore types, many mesopores (intraP pores) can be detected in the Sargelu formation, as well as the existence of microcracks. This formation's pores are mostly spherical, indicating the existence of gaseous phases. Such pores, on the other hand, are scarcely visible in the Asmari reservoir. The pores in this shale sample are mostly interP type and are linked together by some microcracks. Microcracks are more prevalent in the Asmari sample than in the Sargelu. Fig. 10 shows the TEM images of the shale rocks (in powder form), where various types of pores and cracks can be seen, similar to the SEM images. Furthermore, the presence of pyrite is seen in the Asmari reservoir (Fig. 10c).

Table 1.
XRF results of Sargelu and Asmari reservoirs.

Concentration (%)	CaO	SiO_2	Fe_2O_3	Al_2O_3	SO_3	K_2O	P_2O_5	MgO	TiO_2	SrO	MoO_3
Sargelu	45.5	20.9	13.4	9.86	4.55	2.11	1.8	1.09	0.53	0.0569	0.052
Asmari	80.46	5.37	9.15	1.4	0.57	0.32	-	1.73	0.19	-	-

5. Conclusions

The Sargelu and Asmari shale reservoirs were investigated in this study in terms of pore characteristics and composition. The findings are described below:

- According to the XRD patterns, the primary components detected in both formations were calcite, quartz, and kaolinite.
- According to the XRF results, the primary components in both samples were CaO, SiO_2, and Fe_2O_3. P_2O_5, SrO, and MoO_3 were only discovered in the Asmari reservoir samples.
- According to the TGA examination, the amount of OM and other possible carbonate components in the Sargelu formation was ~37%, compared to ~40.5% in the Asmari formation.
- The FTIR approach revealed the existence of functional groups C-H, C=O, C-O, Si-O, C-O-O, and C-C in both shale samples, but only O-H and C=C in the Asmari shale.
- Finally, the porosity structure of both shale formations was investigated using several microscopy techniques, including FESEM, FESEM-FIB, FIB-TEM, and TEM, revealing the presence of micropores, mesopores, macropores, and microfractures in both samples.

Acknowledgements

This research was supported by National Research Foundation of Korea (NRF) funded by the Ministry of Science and ICT (2020H1D3A1A04081409 and 2022R1I1A1A01067572).

Conflicts of interest

Authors declare no conflict of interest.

REFERENCES

[1] R.A. Kerr, Natural gas from shale bursts onto the scene, Science 328 (2010) 1624–1626.
[2] M.A. Hanif, F. Nadeem, R. Tariq, U. Rashid, Renewable and Alternative Energy Resources, Elsevier Science, Netherlands, 2021.
[3] J. Cooper, L. Stamford, A. Azapagic, Shale Gas: A Review of the Economic, Environmental, and Social Sustainability, Energy Technology 4(7) (2016) 772-792.
[4] P. Liu, Y. Feng, L. Zhao, N. Li, Z. Luo, Technical status and challenges of shale gas development in Sichuan Basin, China, Petroleum 1 (2015) 1-7.
[5] J. Bellani, H.K. Verma, D. Khatri, D. Makwana, M. Shah, Shale gas: a step toward sustainable energy future, Journal of Petroleum Exploration and Production Technology 11(5) (2021) 2127-2141.
[6] A. Striolo, D.R. Cole, Understanding Shale Gas: Recent Progress and Remaining Challenges, Energy & Fuels 31(10) (2017) 10300-10310.
[7] Z. Li, Z. Lei, W. Shen, D.A. Martyushev, X. Hu, A Comprehensive Review of the Oil Flow Mechanism and Numerical Simulations in Shale Oil Reservoirs, Energies 16(8) (2023) 3516.
[8] M. Josh, L. Esteban, C. Delle Piane, J. Sarout, D.N. Dewhurst, M.B. Clennell, Laboratory characterisation of shale properties, Journal of Petroleum Science and Engineering 88-89 (2012) 107-124.
[9] D. Feng, Z. Chen, W. Zhao, K. Wu, J. Li, X. Li, Y. Gao, S. Zhang, F. Peng, Determination of Apparent Pore Size Distributions of Organic Matter and Inorganic Matter in Shale Rocks Based on Water and N2 Adsorption, Energy & Fuels 36(19) (2022) 11787-11797.
[10] J. Yang, J. Hatcherian, P.C. Hackley, A.E. Pomerantz, Nanoscale geochemical and geomechanical characterization of organic matter in shale, Nature Communications 8(2179) (2017) 1-9.
[11] K.-Q. Liu, Z.-J. Jin, L.-B. Zeng, M.-D. Sun, B. Liu, H.W. Jang, M. Safaei-Farouji, M. Shokouhimer, M. Ostadhassan, Microstructural analysis of organic matter in shale by SAXS and WAXS methods, Petroleum Science 19(3) (2022) 979-989.
[12] H. Zhang, D.Y. Moh, X. Wang, R. Qiao, Review on Pore-Scale Physics of Shale Gas Recovery Dynamics: Insights from Molecular Dynamics Simulations, Energy Fuels 36 (2022) 14657–14672.
[13] D. Xia, Z. Yang, T. Gao, H. Li, W. Lin, Characteristics of micro- and nano-pores in shale oil reservoirs, Journal of Petroleum Exploration and Production 11(1) (2021) 157-169.
[14] P. Zhang, S. Lu, J. Li, H. Xue, W. Li, P. Zhang, Characterization of shale pore system: A case study of Paleogene Xin'gouzui Formation in the Jianghan basin, China, Marine and Petroleum Geology 79 (2017) 321–334.
[15] A. Ghajari, M. Kamali, S. Mortazavi, A comprehensive study of Laffan Shale Formation in Sirri oil fields, offshore Iran: Implications for borehole stability, Journal of Petroleum Science and Engineering 107 (2013) 50–56.
[16] H. Tian, L. Pan, X. Xiao, R. Wilkins, Z. Meng, B. Huang, A preliminary study on the pore characterization of Lower Silurian black shales in the Chuandong Thrust Fold Belt, Southwestern China using low pressure N2 adsorption and FE-SEM methods, Marine and Petroleum Geology 48 (2013) 8–19.
[17] M. Sun, J. Zhao, Z. Pan, Q. Hu, B. Yu, Y. Tan, L. Sun, L. Bai, C. Wu, T.P. Blach, Y. Zhang, C. Zhang, G. Cheng, Pore characterization of shales: A review of small angle scattering technique, Journal of Natural Gas Science and Engineering 78 (2020) 103294.
\[19] P. Tahmasebi, F. Javadpour, M. Sahimi, Three-Dimensional Stochastic Characterization of Shale SEM Images, Transport in Porous Media 110 (2015) 521–531.
[20] P. Zhang, S. Lu, J. Li, H. Xue, W. Li, P. Zhang, Characterization of shale pore system: A case study of Paleogene Xin'gouzui Formation in the Jianghan basin, China, Marine and Petroleum Geology 79 (2017) 321–334.
[21] Y. Wang, Y. Zhu, S. Chen, W. Li, Characteristics of the Nanoscale Pore Structure in Northwestern Hunan Shale Gas Reservoirs Using Field Emission Scanning Electron Microscopy, High-Pressure Mercury Intrusion, and Gas Adsorption, Energy Fuels 28 (2014) 945–955.
[22] Y. Han, D. Kwak, S.Q. Choi, C. Shin, Y. Lee, H. Kim, Pore Structure Characterization of Shale Using Gas Physisorption: Effect of Chemical Compositions, Minerals 7(5) (2017) 66.
[23] K. Liu, M. Ostadhassan, W. Jang, Comparison of fractal dimensions from nitrogen adsorption data in shale via di ferent models, RSC Advances 11 (2021) 2298–2306.
[24] H. Lee, N. Oncel, B. Liu, A. Kukay, F. Altincicek, R.S. Varma, M. Shokouhimehr, M. Ostadhassan, Structural Evolution of Organic Matter in Deep Shales by Spectroscopy (1H and 13C Nuclear Magnetic Resonance, X ray Photoelectron Spectroscopy, and Fourier Transform Infrared) Analysis, Energy Fuels 34 (2020) 2807–2815.
[25] A. Al-Otoom, M. Allawzi, A. Ajlouni, F. Abu-Alrub, M. Kandah, The use of oil shale ash in the production of biodiesel from waste vegetable oil, Journal of Renewable and Sustainable Energy 4 (2012) 063123.
[26] M.A. Rahman, T. Oomori, Structure, crystallization and mineral composition of sclerites in the alcyonarian coral, Journal of Crystal Growth 310 (2008) 3528–3534.
[27] A.F. Muhammad, M.S. El Salmawy, A.M. Abdelaala, S. Sameah, El-Nakheil oil shale: Material characterization and effect of acid leaching, Oil Shale 28 (2011) 528–547.
[28] A. Negahdari, M. Ziaii, J. Ghiasi-Freez, Application of discriminant analysis for studying the source rock potential of probable formations in the Lorestan basin, International Journal of Mining and Geo-Engineering 48 (2014) 31-54.
[29] A. Maleki, M.H. Saberi, S.A. Moallemi, M.H. Jazayeri, Evaluation of hydrocarbon generation potential of source rock using two-dimensional modeling of sedimentary basin: a case study in North Dezful Embayment, Southwest Iran, Journal of Petroleum Exploration and Production Technology 11 (2021) 2861–2876.
[30] A. Shekarifard, Thermochemical analysis of the oil shale, from the Middle Jurassic Sargelu Formation, Southwest Iran: A thermo-oxidative approach, Geopersia 12(1) (2022) 127-139.
[31] A. Seyrafian, Microfacies and depositional environments of the Asmari formation, at Dehdez area (a correlation across Central Zagros Basin), Carbonates Evaporites 15 (2000) 121–129.
[32] M. Moradi, R. Moussavi-Harami, A. Mahboubi, M. Khanehbad, A. Ghabeishavi, Rock typing using geological and petrophysical data in the Asmari reservoir, Aghajari Oilfield, SW Iran, Journal of Petroleum Science and Engineering 152 (2017) 523–537.
[33] M.R.M. Fereidoni, M. Lotfi, N. Rashid nejad, Evaluate geochemical trace elements of Qalikuh oil shale (Southwest Aligoodarz) using elemental analysis and rock eval pyrolysis, Scientific Quarterly Journal of Geosciences 25 (2016) 171–180.
[34] V. Zarei, A. Nasiri, Stabilizing Asmari Formation interlayer shales using water-based mud containing biogenic silica oxide nanoparticles synthesized, Journal of Natural Gas Science and Engineering 91 (2021) 103928.
[35] K. Shimokawa, N. Ima, M. Hirota, Dating of a volcanic rock by electron spin

resonance, Chemical Geology 46 (1984) 365–373.
[36] C.B. Azzoni, D.D.I. Martino, C. Chiavari, E. Sibilia, M. Vandini, Electron paramagnetic resonance of mosaic glasses from the Mediterranean area, Archaeometry 4 (2002) 543–554.
[37] B. Khani, M. Kamali, M. Mirshahani, M. Memariani, M. Bargrizan, Maturity modeling and burial history reconstruction for Garau and Sargelu formations in Lurestan basin, south Iran, Arabian Journal of Geosciences 11 (2018) 39.
[38] N.E. Altun, C. Hicyilmaz, J.Y. Hwang, A.S. Bagci, Beneficiation of Himmetoğlu oil shale by flotation as a solid fuel substitute. Part 1. Materials characteristics and flotation behavior, Energy Fuels 20 (2006) 214–221.
[39] B. Chen, X. Han, X. Jiang, In-situ FTIR analysis of the evolution of functional groups of oil shale during the pyrolysis, Energy Fuels 30 (2016) 5611–5616.
[40] Y. Wang, Y. Zhu, H. Wang, G. Feng, Nanoscale pore morphology and distribution of lacustrine shale reservoirs: Examples from the Upper Triassic Yanchang Formation, Ordos Basin, Journal of Energy Chemistry 24 (2015) 512–519.